

# Nanoparticles: Production, Characterization and Applications

L. Torrisi<sup>1</sup>, A. Cassisa<sup>1</sup>, L. Silipigni<sup>1</sup>, M. Cutroneo<sup>2</sup> and A. Torrisi<sup>2</sup>

<sup>1</sup>*Dipartimento di Scienze Fisiche MIFT, Università di Messina, Italy*

<sup>2</sup>*Nuclear Physics Institute, CAS, 25068 Rez, Czech Republic*

## Abstract

The production of metallic nanoparticles using pulsed laser ablation in water is presented. The physical characterization of the produced nanoparticles is reported in terms of electronic microscopy, optical and mechanical properties, SPR, EDX, XPS and XRD spectroscopies.

The applications of the prepared nanoparticles involve different scientific fields. In particular will be discussed their use to modify some properties of polymers, liquids and alloys. Special attention is devoted to the use of nanoparticles for polymeric laser welding, to the use as an image contrast medium in the biological environment and to the use of Au-NPs targeting for radiotherapy of cancer tissues.

**Corresponding Author:** lorenzo.torrisi@unime.it

**Keywords:** Nanoparticles; surface plasmon resonance; surface analysis; radiotherapy; hyperthermia.

## 1. INTRODUCTION

In the last 10 years more and more nanoparticles (NPs) production, characterization and applications play important role in the development of new materials, image diagnostic techniques and bio-medical, chemical and physical applications.

Nanostructured materials have high interest due to their specific chemical and physical properties changing with the use of different nanoparticle concentration. Very interesting properties can be attributed to the high surface/volume ratio of the employed nanoparticles embedded or deposited on other materials. For example, the wetting ability of different surfaces can be modified using a nanoparticle thin film deposited on them [1]. Polymers, ceramics and metals are modified by the presence of nanoparticles embedded in their matrices. For example, the optical, electrical, thermal and mechanical properties of many polymers can be modified using 1% wt. concentration or less of metallic nanoparticles embedded in the polymer [2].

Nanoparticles using heavy metals and ferromagnetic materials can be employed as a contrast medium to better acquire images of special compounds of interfaces or biological tissues in which the nanoparticles have been injected [3].

The presence of nanoparticles in cancer tissues enhances the energy released by ionizing radiations to the tissue permitting to deposit higher doses and to damage the cell's DNA inducing apoptosis and arrest of tissue proliferation [4].

The use of metallic nanoparticles in cancer tissue promotes the resonant light absorption enhancing the tissue temperature under illumination and permitting localized hyperthermia [5].

Nanoparticles, through colloidal chemistry in liquid environments, play a role in many processes in nature, in industrial processes, such as the synthesis of glasses, the optical and electrical properties of thin films and the useful applications in the biomedicine field. Typical colloids are representative of nanoparticles stabilized in solution in order to prevent aggregation. The stabilization, in general, takes place by the absorption of electric charges on the surface, leading to a repulsion of the nanoparticles as long as a critical distance is maintained [6].

In the present paper, various aspects of nanoparticles are discussed, showing the fabrication of novel materials with specific applications that can be presented in the actual market.

## 2. EXPERIMENTAL SET-UP

An Nd:YAG laser operating at 1064nm (fundamental wavelength), with 3 ns pulse duration, 300 mJ maximum pulse energy of 300 mJ, 10 Hz maximum repetition rate, was employed and  $10^{10}$  W/cm<sup>2</sup> intensity was employed in this experiment. The laser is focused on metallic pure targets (Au, Ag, Ti,...) placed in water at 5 mm depth of distilled water using 1 mm<sup>2</sup> spot size.

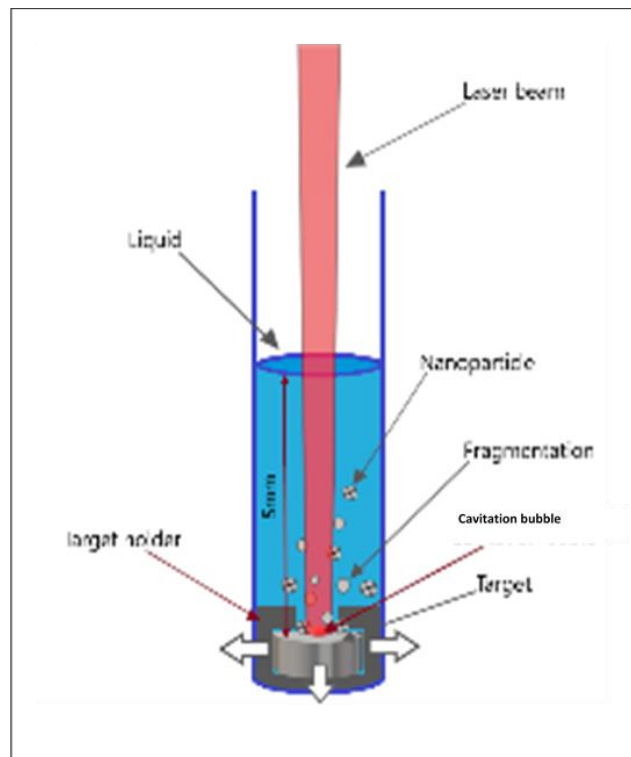


**Fig. 1:** Experimental set-up used for the production of nanoparticles by laser ablation in water.

Figure 1(a) shows a typical set-up for the particle preparation by laser ablation in water. The laser light crosses 5 mm water before to arrive at the target. The interaction produces a plasma at the solid-liquid interface, an expanding bubble of ionized gas and its implosion generating the formation of nanoparticles in the liquid. The ablation rate, in terms of ablated mass per laser shot ( $\mu\text{g}/\text{pulse}$ ), is evaluated by the target mass lost after a prolonged irradiation time and is obtained using a micrometric balance, as reported in previous experiments [7]. The target holder permits little movements of the target during the laser ablation process due to the shock waves pressure.

This movement is useful to irradiate a large area ablation of the target without generating a deep cratered.

The control of the laser parameters (pulse energy and spot size) and irradiation time (5 min-50 min) at 10 Hz repetition time permit to generate a solution with a different concentration of nanoparticles. Generally, concentrations within 0.1 mg/ml up to 10 mg/ml are prepared.

In order to stabilize the solution avoiding particle aggregation, a surfactant at low concentration (1  $\mu\text{g/ml}$ ) is employed, according to the literature [8].

The measure of nanoparticle shape, size and aggregation type are performed using electron microscopy (SEM and TEM). Optical absorbance analysis was obtained using spectrophotometers operating in the visible wavelength range. Wetting ability measurements were obtained using a suitable optical microscope permitting the evaluation of the contact angle of 1  $\mu\text{l}$  water drop deposited on the substrate surface near a cross-sectioned zone, according to the literature [1].

The evaluation of the absorbed dose in biological tissues containing metallic nanoparticles was obtained using the massive absorption coefficients and the electron and ion stopping powers and ranges given by NIST database [9, 10].

### 3. RESULTS

#### 3.1 Nanoparticles Characterization

The properties of a nanoparticle are bonded to the particle composition, size and shape, and in particular to the number of exposed atoms at its surface. The increment of the surface area with respect to the volume represents an important parameter to enhance the surface effects. For a nanoparticle, for example, it involves the surface properties such as the wettability, electrical behavior, optical absorption, adhesiveness, chemical reactivity, mechanical resistance, and others.

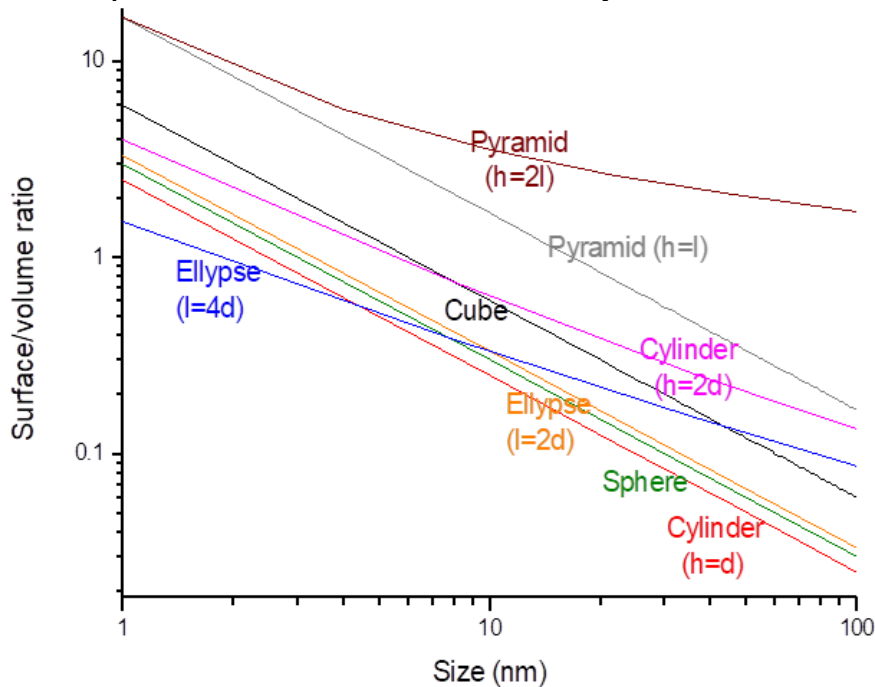


**Fig. 2:** Surface /volume ratio versus the nanoparticle size (main length) dependence.

The smaller a particle the larger the fraction of atoms at its surface, and the higher the average binding energy per atom. The surface-to-volume ratio ( $S/V$ ) scales with the inverse size, and therefore, there are numerous properties that obey the same scaling law. As an example, Fig. 2 reports the surface/volume ratio as a function of the nanoparticle size (main length of the solid shape). As representative of the main solid shape was chosen the side length for the cube, the diameter length for sphere, the height length for the cylinder (equal or double with respect to the base diameter), the maximum length for ellipsoid (maximum axes double or quadruple of the transversal axes), the height of a pyramid with a triangular base with equal sides (height equal or double with respect to the triangle side). Fig. 2 demonstrates an increment of the surface/volume ratio decreasing the nanoparticle size and a maximum  $S/V$  values for the pyramid shape. In agreement with the literature [11], the surface increment with respect to the volume of smaller particles indicates that their use may amplify some characteristics dependent by their surface. For instance, one advantage to use nanoparticles in liquid solutions or deposited on a solid surface consists in the increment of the surface wetting ability: the nanoparticles decreases the cohesion forces inside the liquid solution containing them and increase the adhesion forces at the solid-liquid interface.

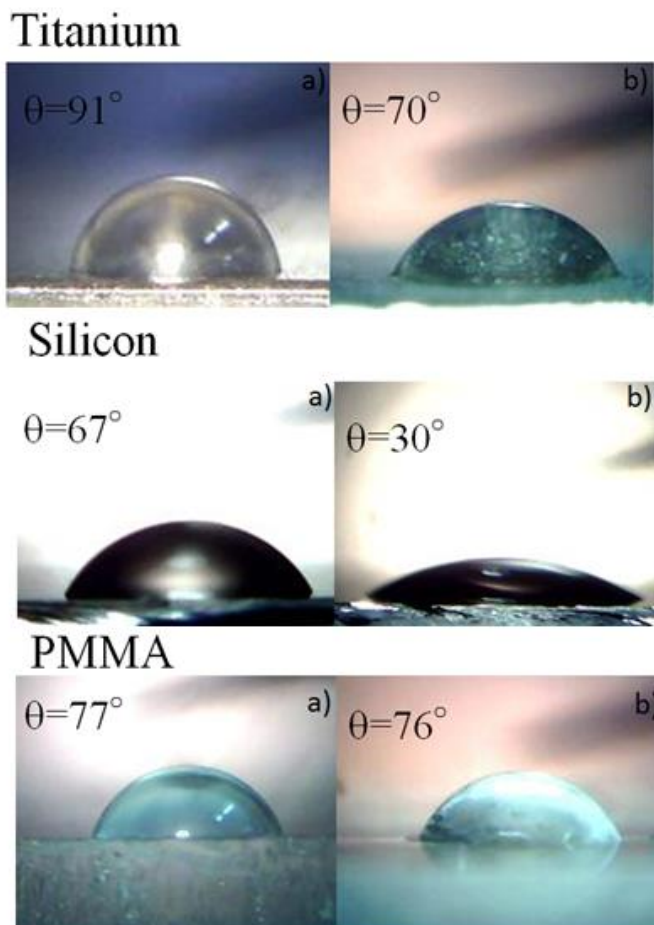


**Fig. 3:** Contact angle measurements of distilled water on the pure substrate (a) and on the substrate on which some monolayers of nanoparticles of Au-NPs are deposited (b).

Fig. 3 reports a comparison of some contact angle measurements of liquids solutions (distilled water) deposited as a micrometric drop on different clean and flat solid surfaces (Ti, Si and PMMA) (a). The optical microscope measurements demonstrate that Au-NPs present on the first monolayers of the solid surface decrease the contact angles with respect to the value measured without nanoparticle, resulting an improving of the wetting ability of the solution to the substrate (b), in agreement with the literature [12].

The laser produced nanoparticles are submitted to a physical characterization in order to distinguish their properties, size, composition, type of generated solution (concentration, color, density, optical absorbance vs. wavelength,...) and time and temperature dependence of the solution (nanoparticle aggregation with the time and with the temperature increment, stabilization using different surfactants,...).

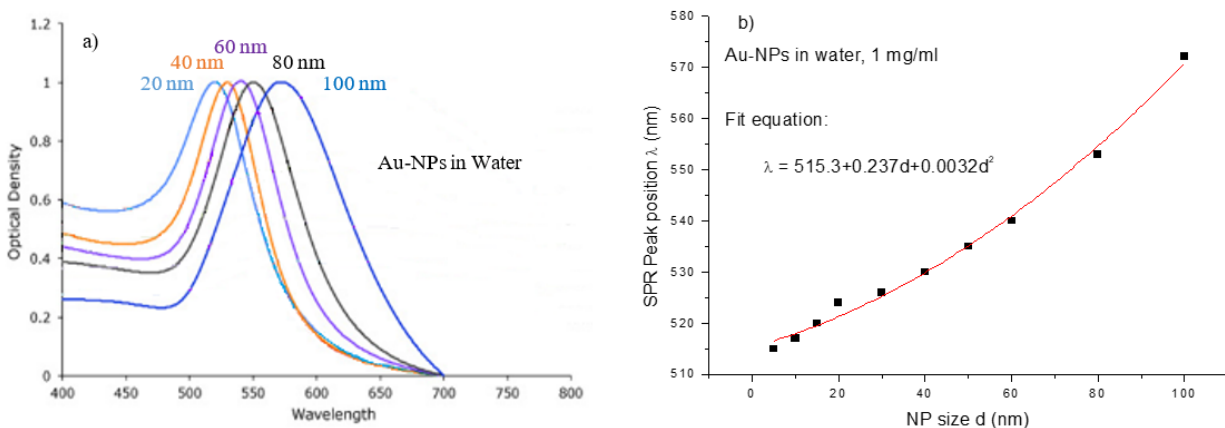


**Fig. 4:** Absorbance of Au-NPs in water versus wavelength and NP size (a) and SPR peak position versus NP size (b).

Fig. 4a reports a typical normalized optical absorbance measurement of Au-NPs as a function of the wavelength and of the nanoparticle size. The metallic nanoparticles promote the surface plasmon resonance (SPR) absorption effect when they are illuminated by light in particular wavelength bands [13]. In fact, they become an induced electric dipole by the incident electromagnetic light and at the electron plasmon resonance the disruptive interference coupling reduces significantly the intensity of the incident intensity light. The absorbance SPR bands are peaked at about 520 nm for Au-NPs with 20 nm diameter and shift towards higher wavelengths increasing the nanoparticle size, according to the literature [14]. A study of this shift vs. NPs size demonstrates that the trend is quadratic exponential with the NP size, as reported in the plot of Fig. 4b containing also the fit equation of the experimental data.

The TEM microscopy of the produced nanoparticles is indispensable to evaluate the NPs shape and their size distribution, in fact, not all particles have the same distribution but an average value and a standard deviation can be given. Moreover, the electron microscopy permits to observe if nanoparticles are separated or if effects of nanometric aggregations and formation of micrometric grains are generated.

Fig. 5 reports four typical examples of TEM images of Au-nanospheres with an average diameter of 25 nm (a), of polystyrene nanoellipses with an average main axes of 800 nm (b), of Au-nanorods with an average length of 200 nm (c) and of Ni-nanopyramids with an average high of 20 nm (d).

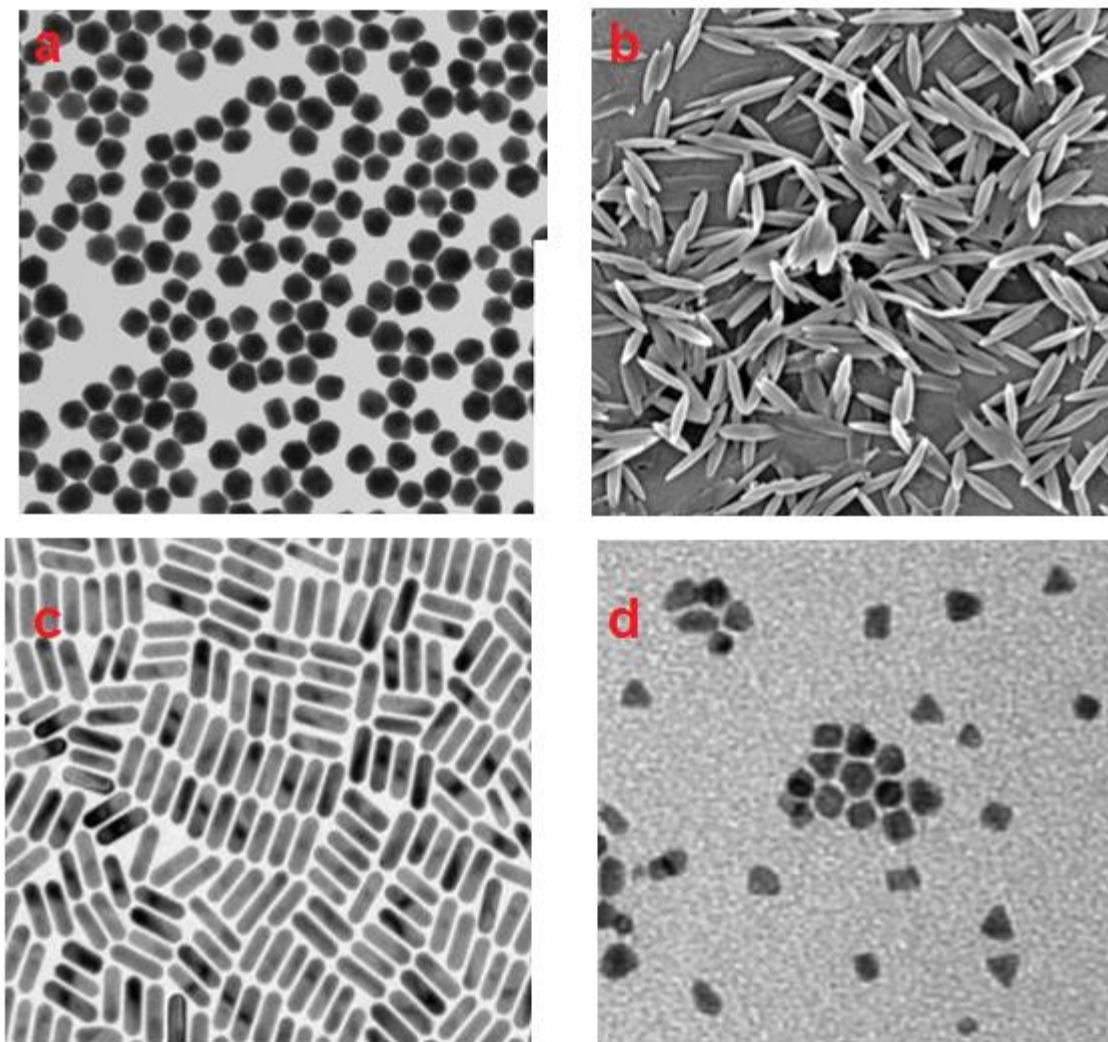


**Fig. 5:** TEM microscopy of Au-nanospheres (a), polystyrene-nanoellipsoids (b), Au-nanorods (c) and Ni-nanopyramids (d).

### 3.2 Nanoparticles applications

The introduction of nanoparticles in polymers represents a simple process performed at the melting temperature of the polymer in which liquid can be added the nanoparticles at different concentration. The solution, after a suitable hot mixing, is slowly cooled to generate the solid polymer uniformly enriched by the nanoparticles. Such procedure permits to generate polymers with very different properties from the pristine ones. Synthesized polymers, for instance, can have a different color, density, electrical, optical and mechanical properties.

An example of such procedure was used for carbon nanotubes (CNT) embedded uniformly in polyethylene (type UHMWPE) in order to change significantly its optical and electrical properties. In addition, the very low concentration of CNT, of the order of 0.1%, alter the polymer properties. Fig. 6a reports a typical curve of the measured absorption coefficient at 532 nm wavelength as a function of the CNT concentration. This result finds immediate applications in the field of polymer welding by laser or by lamps. The pristine UHMWPE is transparent to the visible light and the

visible radiation is poorly absorbed and transmitted even at great depth. The CNT doped polymer produces a black material strongly absorbent the visible light in the first sub-microns layers depth.

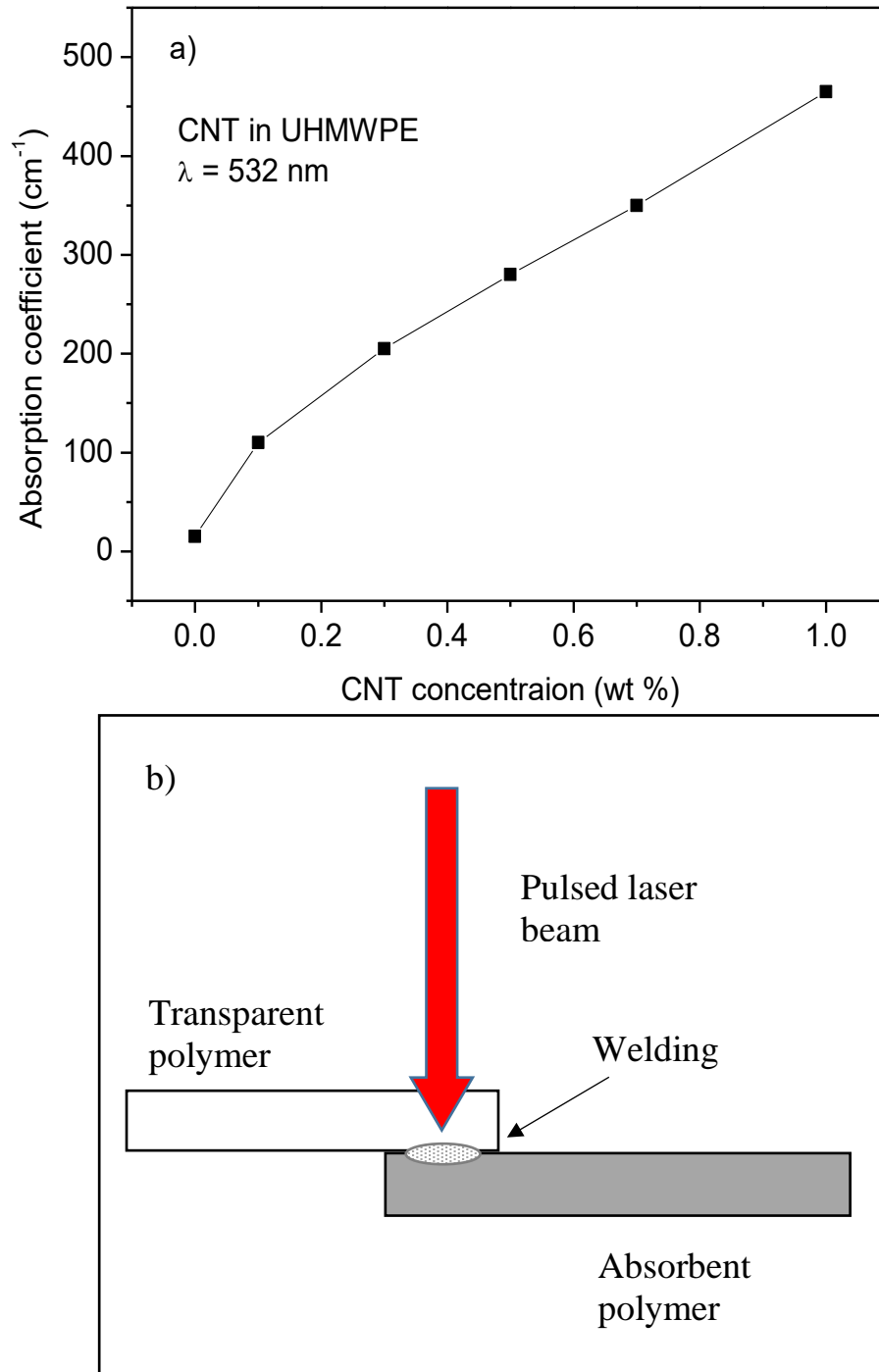


**Fig. 6:** Absorption coefficient at 532 nm wavelength in UHMWPE versus CNT concentration (a) and scheme of the laser welding of transparent and absorbent polyethylene foils (b).

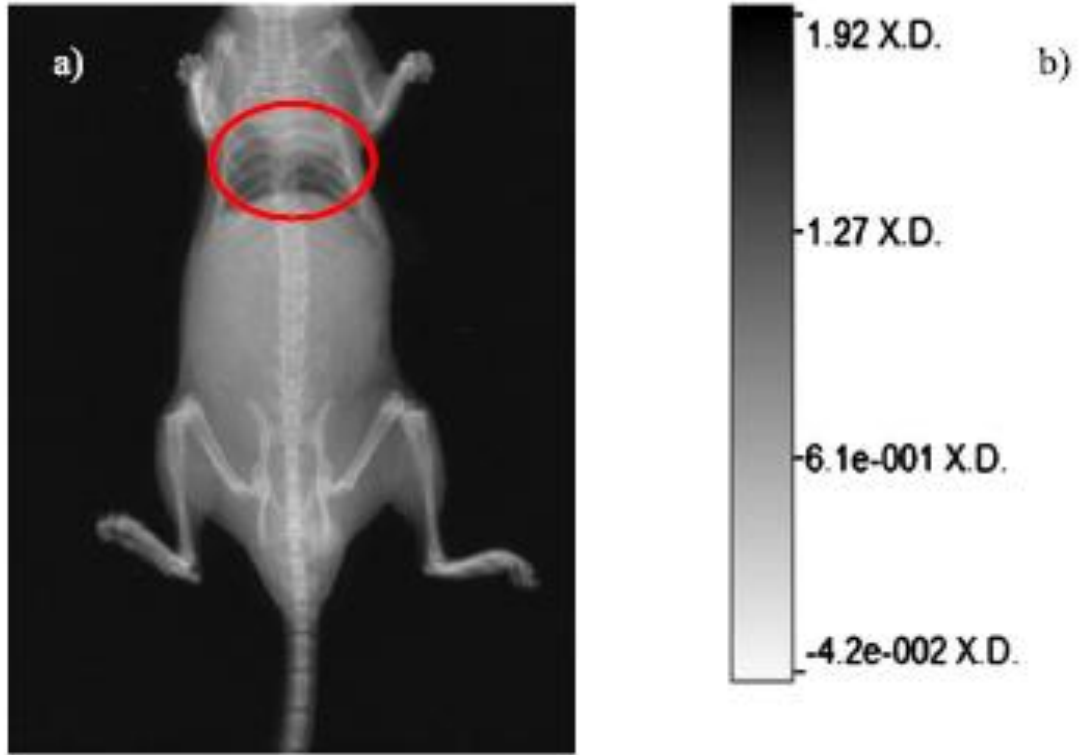


**Fig. 7:** X-ray fluorescence image of the Au-NPs in the heart of a mouse (a) and corresponding gray scale intensity (b).

Thus, the coupling foils transparent/black UHWPE layers can be irradiated by laser pulse beams crossing the transparent one and producing a high-energy deposition at the interface between the two polymers. This process produces a confined micrometric plasma in which the temperature is so high to melt both polymers and to induce their mixing and foil welding by the cooling process, i.e. just the laser pulse finish or is shifted to the next places. Fig. 6b reports a scheme of the laser welding process based on the CNT particles embedded in the UHMWPE polymer. More details on this application are reported in the literature [2].

The imaging contrast agent may be employed to enhance differentiation between two tissue types or to highlight disease-specific anatomical features or functional processes at the molecular, cellular, or tissue level. Many types of contrast medium exist and can be used for different diagnostics; for instance, ferromagnetic nanoparticles can be used for NMR images, while Gd, I, Au and Bi for X-ray CT images. For low X-ray energy the photoelectric effect take place and the attenuation coefficient  $\mu$  is described by the following equation:

$$\mu = \rho Z^4/AE^3 \quad (1),$$

where  $\rho$  is the density,  $Z$  is the atomic number,  $A$  is the atomic mass, and  $E$  is the X-ray energy. Thus,  $\mu$  is very high if heavy elements are irradiated at energy promoting photoelectric effects, such as for Mammography and CT images (10-60 KV).

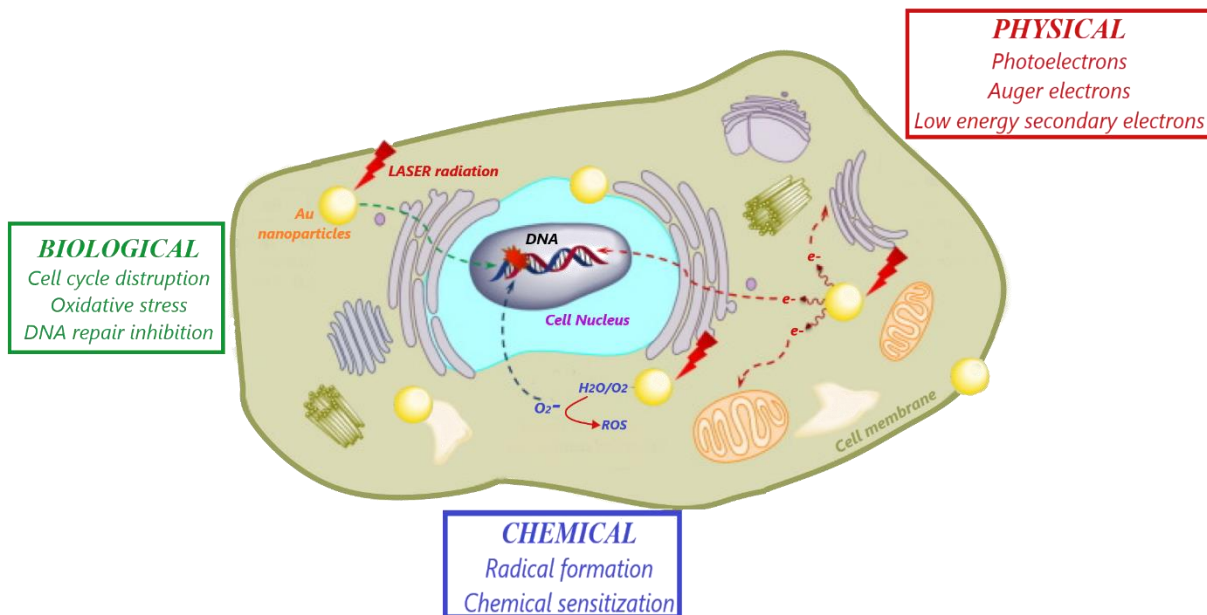
Using the K-edge absorption of gold, the detection of contrast agents using measurements of their characteristic X-ray attenuation profiles, has been used to detect Au-NP in vivo, permitting to localize the tissues containing the nanoparticles with a contrast depending on their concentration, visualizing interfaces, liquids, special tissues and diseased organs with a high spatial resolution. The Au-NPs are biocompatible, stable and injectable also at high concentration (1-10 mg/ml).

Fig. 7 reports a typical X-ray image of Au-NPs injected in the blood flux of a mouse and acquired after 10 m of injection at which the uptake in the heart has a maximum value. After this time, the uptake decreases in heart and growth in other organs. More details on these image acquisitions using Au-NPs contrast medium are reported in the literature [15].

The benefices of the Au and Bi-NPs, and of other biocompatible, heavy and stable nanoparticles, can be used to be obtain not only high contrast image diagnostics but also for radiotherapy improvements. The introduction of Au-NPs in tumor cells permits to modify the electron density of the cell [16]. The Au-NPs from the extracellular liquid in which are injected may cross the cell membrane, especially if bound to proteins or other functionalized molecules useful for the cell life, diffuse in the cytoplasm medium and arrive at the nucleus, i.e. near to the DNA and RNA, the important vital parts of the cell. Here the Au-NPs enhances the atomic number effective of the nucleus and, if invested by energetic ionizing radiations, such as photons, electrons and ions, produces high effects of ionization, emission of energetic electrons and presence of ions and reactive radicals. These non-equilibrium conditions, associated with the presence of high-energy release in the environment around to the metallic nanoparticle, may produce damage of DNA and RNA with consequent cell death. Thus, if the Au-NPs have reached the nucleus of cancer cells, the exposition to radiotherapy may generate high-absorbed doses to destroy the cells.

Based on this idea, Au-NPs in solutions can be injected into living organisms to be transported selectively in the cancer cells and not in the healthy ones. This action is the most difficult to realize because the NPs tend to diffuse in any cells, however, the major blood spraying in the cancer cells enhances their Au-NPs presence with respect to the healthy ones. Moreover, the direct injection of the solution containing Au-NPs in the tumor tissue. This action, monitored by contrast images, can be followed by adapt radiotherapy using X-rays or electrons or ion beams, delimiting the irradiated zone and increasing the deposited radiation dose to the tumor site. The presence of the Au-NPs, generally at concentrations of the order of 1-10 mg/ml, enhances the absorbed dose and the consequent damage to the cells in which Au-NPs have been introduced.

Fig. 8 reports a general scheme of a cell structure, delimited by its membrane, of about 10 nm thick, of the inner cytoplasm solution containing many biomolecules such as proteins and nucleic acids, the organelles and the nucleus. Here the DNA is organized in one or more linear molecules, called chromosomes, which are associated with histone proteins. All chromosomal DNA is stored in the cell nucleus, separated from the cytoplasm by a membrane. The ionizing radiations hitting the cells, has a high probability to damage irreparably the DNA if Au-NPs are incorporated in the cell, due to energetic photons, electrons and ions inducing ionization, secondary photoelectrons, Auger electrons, molecular scissions, hydrolysis, reactive radicals, heat and charge species formation. Thus, is expected that the presence of Au-NPs enhances significantly the absorbed doses and the damage to the vital DNA and to the entire cell, improving the radiotherapy efficiency against the cancer cells.



**Fig. 8:** Cell scheme indicating the Au-NPs introduced in the cytoplasm and the effect of the radiotherapy producing radiations damaging the vital DNA.

#### 4. CONCLUSIONS

In conclusion, nanoparticles of different elements can be prepared using the technique of the pulsed laser ablation in water, a simple cheap and clean method of preparation. Ferromagnetic, heavy metals and biocompatible nanoparticles can be prepared in a liquid solution, which concentration depends mainly by the laser ablation yield and by the laser irradiation time.

The prepared solution may be characterized in terms of the type of nanoparticles, size and shape, stability, concentration and biocompatibility before to be employed for different scopes.

There are many possible applications of the prepared solutions. One of these concerns the possibility to be used to embed the NPs in different materials in order to change their physical and chemical properties. Polymers, for example, change their properties if nanoparticles are embedded also at low concentrations, modifying their color, optical absorbance and transmittance, mechanical resistance, electrical and thermal conduction and chemical reactivity. Nanoparticles can be deposited as monolayers or thin film on different substrates, modifying the surface properties, such as reflection and absorption, wetting ability, adhesion interface, roughness, work function and surface reactivity.

The prepared solutions can be also injected *in vitro* and *in vivo* in biological environments to study their diffusion, fluid dynamics, uptake and decay and formation of concentration gradients. The nanoparticle information can be obtained using them as a contrast medium in X-ray images, such as occurs for Au-NPs injected in living mice, permitting to measure the uptake of the trace element in different organs in presence of health or disease state.

Finally, heavy biocompatible elements nanoparticle, such as Pt, Au and Bi-NPs, with specific functionalized molecules, can be employed to be injected in the extracellular liquid, to diffuse up to the cell membrane, and to cross the membrane arriving near to the nucleus of cancer cells. Their accumulation determines the growth of concentration adapts to enhance the radiotherapy treatment. The high electron density, in fact, determines a higher linear energy transfer (LET) from

the incident ionizing radiation to the biological environment with an increment of the radiation damage to vital organs of the cell, such as to DNA, which produces the cell death. At the actual stage, the major difficulty is to introduce the heavy nanoparticles for radiotherapy only in the tumor cells and not in the healthy ones.

### Acknowledgements

This work was supported by the “Research and Mobility” project of Messina University No. 74893496, scientifically coordinated by Professor L. Torrìsi.

The research has been realized at the CANAM (Center of Accelerators and Nuclear Analytical Methods) infrastructure LM 2015056 and has been supported by project GACR No. 16-05167S.

### References

- [1] L. Torrìsi, C. Scolaro and N. Restuccia,  
Wetting ability of biological liquids in presence of metallic nanoparticles,  
*Journal of Materials Science: Materials in Medicine* (2017) 28: 63-74.
- [2] A. M. Visco, V. Brancato, L. Torrìsi & M. Cutroneo  
Employment of Carbon Nano Materials for the Welding of Polyethylene Joints with a Nd:YAG Laser,  
*International Journal of Polymer Analysis and Characterization* 19: 489–499, 2014.
- [3] C. Rùmenapp, B. Gleich and A. Haase,  
Magnetic Nanoparticles in Magnetic Resonance Imaging and Diagnostics,  
*Pharm. Res.* (2012) 29:1165 –1179.
- [4] L. Torrìsi,  
Radiotherapy Improvements by Using Au Nanoparticles,  
*Recent Patents on Nanotechnology*, 2015, 9(2), 114-125.
- [5] P. Kaur, M.L. Aliru, A.S. Chadha, A. Asea, and S. Krishnan,  
Hyperthermia Using Nanoparticles – Promises and Pitfalls,  
*Int. J. Hyperthermia*. 2016; 32(1): 76–88.
- [6] F. Mafuné, J. Kohno, Y. Takeda, and T. Kondow, H. Sawabe,  
Formation of Gold Nanoparticles by Laser Ablation in Aqueous Solution of Surfactant,  
*J. Phys. Chem. B*, 2001, 105 (22), 5114–5120.
- [7] L. Torrìsi and A. Torrìsi,  
Laser ablation parameters influencing gold nanoparticle synthesis in water,  
*Rad. Eff. And Def. In Solids*, 173:9-10, 729-739, 2018.
- [8] A. Das, R. Chadha, N. Maiti, and S. Kapoor,  
Role of Surfactant in the Formation of Gold Nanoparticles in Aqueous Medium,  
*Journal of Nanoparticles 2014*, Article ID 916429, 1-7.
- [9] NIST - X-Ray Mass Attenuation Coefficients, actual website 2019:  
<https://www.nist.gov/pml/x-ray-mass-attenuation-coefficients>
- [10] NIST - Stopping-Power & Range Tables for Electrons, Protons, and Helium Ions, actual website 2019:  
<https://www.nist.gov/pml/stopping-power-range-tables-electrons-protons-and-helium-ions>
- [11] E. Roduner, Size matters: why nanomaterials are different,

- Chem. Soc. Rev.* 2006, 35 , 583–592.
- [12] L. Torrisi and C. Scolaro,  
Nanoparticles improving the wetting ability of biological liquids,  
*Journ. of Thermodynamics & Catalysis* 8(2), (2018).
- [13] M. A. Garcia. Surface plasmons in metallic nanoparticles: Fundamentals and applications.  
*J Appl Phys* 2011; 44: 283001-19.
- [14] L. Torrisi, N. Restuccia and I. Paterniti,  
Gold Nanoparticles by Laser Ablation for X-Ray Imaging and Protontherapy  
Improvements,  
*Journ. of Thermodynamics & Catalysis*, 2018, 12, 59-69.
- [15] L. Torrisi and N. Restuccia  
Laser-Generated Au Nanoparticles for Bio-Medical Applications  
*IRBM*, on line 2018. <https://doi.org/10.1016/j.irbm.2018.09.005>
- [16] L. Torrisi, L. Silipigni, N. Restuccia, S. Cuzzocrea, M. Cutroneo, F. Barreca, B. Fazio,  
G. Di Marco, S. Guglielmino,  
Laser-generated bismuth nanoparticles for applications in imaging and radiotherapy,  
*Journal of Physics and Chemistry of Solids* 119 (2018) 62-70.